JOURNAL OF MATERIALS SCIENCE 32 (1997) 4585–4589

The relationship between crystal misorientation and conductive mode contrast of grain boundaries in additive-free zinc oxide

J. D. RUSSELL, D. C. HALLS*, C. LEACH
Manchester Materials Science Centre, University of Manchester and University of Manchester Institute of Science and Technology, Grosvenor Street, Manchester M1 7HS, UK
**Department of Materials, Imperial College of Science, Technology and Medicine, Prince Consort Road, London SW7 2BP, UK*

Grain boundaries in additive-free ZnO show different types of conductive mode contrast, depending on the electrical properties. Electron beam scattering patterns have been used to determine the misorientation of grain boundaries showing certain types of conductive mode contrast in order to correlate electrical properties with grain-boundary structure. No correlations were apparent using the coincident-site lattice model, but other criteria suggest that grain-boundary electrical properties may be crystallographically controlled. More detailed analysis will require the full determination of the grain-boundary plane.

1. Introduction

Zinc oxide is an important technological material in the electronics industry and is the main component of polycrystalline varistor devices, which show highly non-ohmic current–voltage characteristics; when subjected to high-voltage transients, the resistance decreases drastically. It is this characteristic together with their ease of fabrication and ability to absorb energy which has made them so attractive to the industry for overvoltage protection for the past 25 years.

The non-ohmic electrical properties of zinc oxide are grain boundary controlled with each grain boundary breaking down at a specific voltage, usually between 2 and 4 V [1]. Studies have been carried out on how different additives and processing routes affect the overall performance of the varistor material which in turn determines the microstructure of the material. This performance is usually measured as a coefficient of non-linearity, α. Process engineers strive to increase this value and coefficients with values between 50 and 100 are not uncommon. Most development work, however, has been based on average properties, and a factor widely overlooked in varistor technology is the way in which individual grain orientations affect the electrical properties at the grain boundaries.

A previous study on additive-free ZnO ceramics using the conductive mode (CM) technique [2] showed the presence of adjacent bright and dark line contrast indicative of double Schottky barriers at certain grain boundaries. Other work has shown that, under similar conditions, single bright or dark lines are observed at other grain boundaries [3]. In this paper, conductive mode images of both types of contrast are combined with electron back-scattering pattern (EBSP) measurements of grain pairs, to investigate whether there is a relation between the crystal misorientation of adjacent grains and the CM contrast which they display. Special boundaries such as coincident-site lattice (CSL) boundaries are sought, together with some other crystallographic measures of boundary mismatch.

Previous researchers have investigated the effect that grain-boundary orientation has on the distribution of dopants and hence on the formation of electrically active interfaces in semiconductor and ceramic materials. For example, in semiconducting MnZn ferrites, boundaries have been classified as either "general" or "special". Of these, general boundaries are highly resistive owing to the segregation of Ca^{2+} ions and a depletion of Fe^{2+} ions. Special or CSL boundaries do not exhibit a strong segregation and are less resistive [4]. Current–voltage measurements of charged grain boundaries in n-Ge bicrystals [5] with $\Sigma = 11$ and $\Sigma = 9$ low-energy symmetric tilt boundaries showed that potential barriers were only found at $\Sigma = 11$ boundaries. Electron-beam-induced current (EBIC) and conductance measurements of both polycrystalline and bicrystalline silicon have been related to crystal orientation by Bary *et al.* [6], who showed that particular orientations favoured different segregations of impurities and hence gave varying strengths of EBIC contrast. Poullain *et al.* [7] found a correlation between the electrical activity as determined by EBIC and the crystallographic structure of silicon grain boundaries.

Whilst these studies used transmission electron microscopy to determine grain-boundary geometry, in this work we have used EBSP measurements in the scanning electron microscope which enables a larger number of grain boundaries to be measured more quickly but does not allow the grain-boundary plane

0022–2461

to be obtained easily. EBSP analysis has, in the past, mainly been used in the study of metals but has also been applied to semiconductors [8, 9].

2. Theory

ZnO has the space group $P6_3mc$ with $a = 3.249\,82$ and $c = 5.206\,61$, giving a lattice which is almost hexagonal close packed ($c/a = 1.60$ versus 1.63 for exact close packing). Any two grain orientations can give rise to several equivalent descriptions of the grain misorientation due to the hexagonal symmetry of each grain. Each grain has 12 symmetry-related orientations, giving 144 valid ways of describing the misorientation using axis–angle pair terminology for example. Conventionally, the axis–angle pair which has the lowest rotation angle is chosen and the axis plotted in the standard triangle [10.0]–[21.0]–[00.1] [10].

One description of special grain boundaries which has been extensively studied is the CSL. In the hexagonal system, these are classified into two types: "common" CSLs occur for any value of c/a, e.g. those due to rotations about [001] or 180° rotations about an axis in the $\langle 00.1 \rangle$ plane; "specific" CSLs are observed only for certain values of c/a. In checking for these, it is necessary to select a band of c/a values about the ideal value since some degree of mismatch is assumed to be taken up by grain-boundary dislocations, in a similar way to the Brandon [11] criterion for the maximum allowable misorientation for a grain boundary from a common CSL misorientation.

CSL misorientations are much less common than in the cubic system. A selection of values for the hexagonal system in the range of interest are given in Table I, after [12, 13].

3. Experimental procedure

3.1. Sample preparation

Zinc oxide ceramic pellets were produced by pressing and firing AR grade powders at 1200 °C for 2 h. The pellets were then ground flat and polished on nylon cloth using a water-based slurry of 0.3 μm α-alumina powder. CM imaging was then carried out around different areas of the microstructure using probes adjusted with a micromanipulator inside a scanning electron microscope (Fig. 1) to determine which interfaces showed double Schottky barrier contrast, bright or dark line contrast, or no contrast at all. Several areas were then mapped out for future reference showing all three types of contrast. The sample was then annealed in a furnace, to alleviate surface deformation caused during mechanical polishing and to enable sharper EBSP patterns to be obtained.

3.2. Electron back-scattering patterns

Grain misorientations were determined at interfaces showing the different contrast types by taking EBSPs using the specimen geometry in Fig. 2. The specimen was tilted at 70° to the electron beam, which ensures a high proportion of diffracted back-scattered primaries. The EBSP image is then digitized and the bands in the pattern used to calculate the orientation of the grain at the point of beam impact relative to the specimen coordinates by a software package from HKL Software Vester Allé 11, DK-9500 Hobro, Denmark.

A piece of silicon wafer cleaved along $\{1\,1\,0\}$ was placed alongside the ceramic under study and aligned with a known direction in the microscope. In this way, the sample coordinates could be aligned with the coordinates of the EBSP, and hence the analysis system. The analysis system then produces raw data in the form of the orientation of each grain studied. For our work, orientations of adjacent grains were paired in order to calculate grain-boundary misorientations and other parameters by a specially developed computer program.

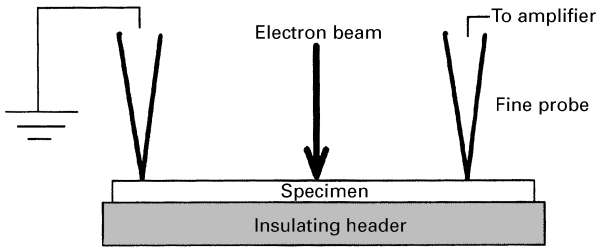

Figure 1 Specimen configuration used for CM analysis of electronic ceramics.

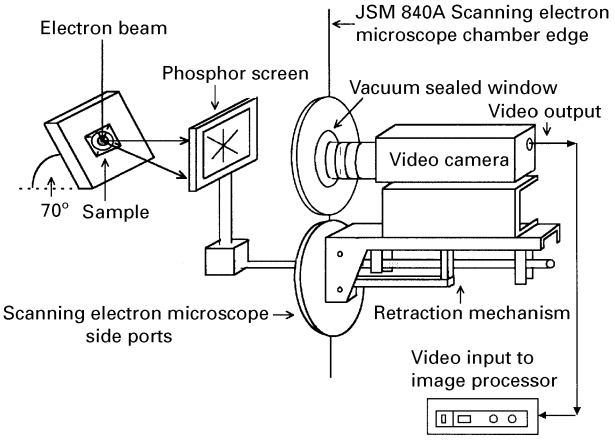

Figure 2 EBSP experimental arrangement.

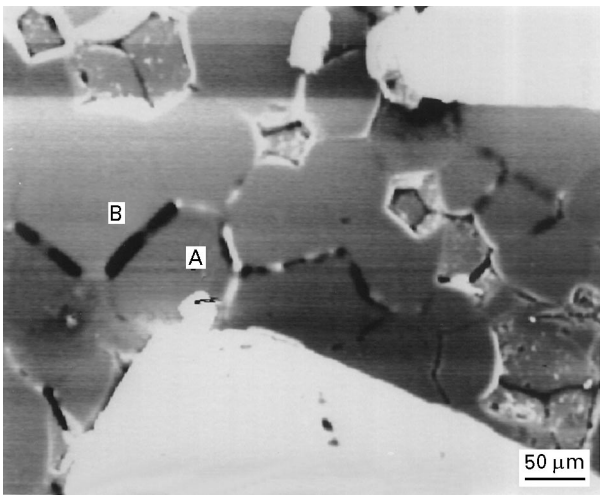

Figure 3 Typical CM image showing type I contrast at A and type II contrast at B.

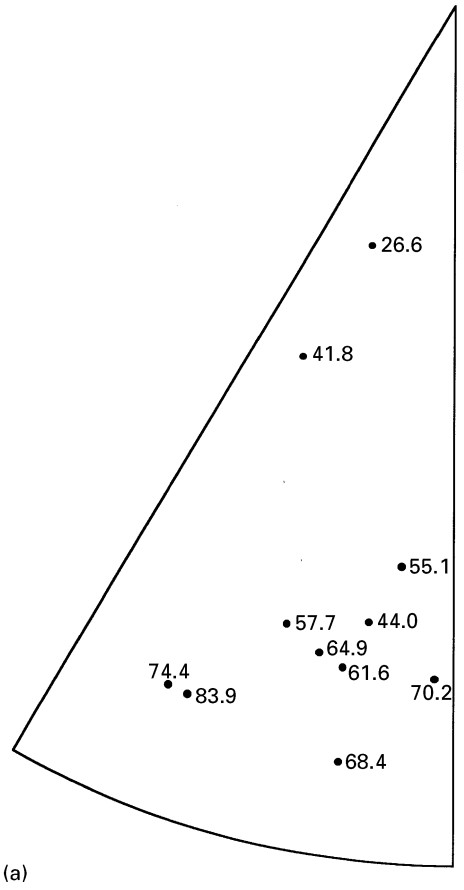

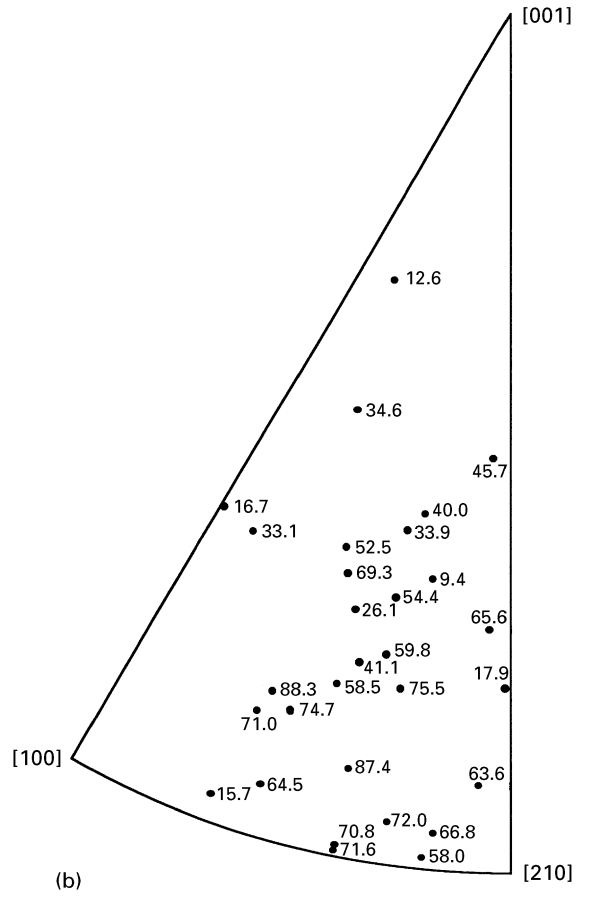

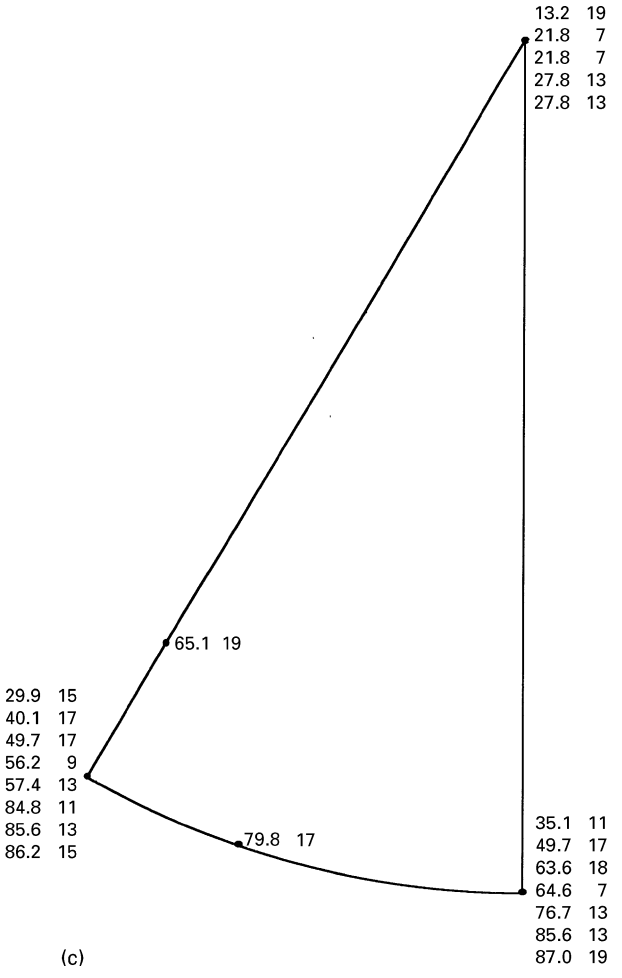

Figure 4 Minimum-angle axis–angle pair distribution for grain boundaries showing (a) type I contrast and (b) type II contrast. (c) The distribution for CSLs with $\Sigma < 20$, and $1.581 < c/a < 1.62$. In each case the dots denote the axis, and the number is the angle in degrees, with the multiplicity added for (c) (see Table I).

4. Results and discussion

A typical CM image is shown in Fig. 3, from which appropriate grain boundaries were identified, and EBSP analysis was carried out on either side. The relative size of the probes and the grains, coupled with the imprecision of movement of the micromanipulators, did not allow adjacent grains to be probed. Moving the probes to various different positions, the contrast was seen to change only in strength, but not in type. Whether the observed contrast is dark or bright depends only on the direction of current flow (reversing the probes inverts the contrast). Some boundaries show no contrast, but in these cases it is often difficult to evaluate whether this is due to properties of the grain boundaries themselves, or to their geometry relative to the probes; for example, if they traverse the direction between the probes, little current might be expected to be collected.

One of the commonest criteria for specialness of grain boundaries is the correlation with CSL boundaries. This approach also has the advantage of not requiring the orientation of the grain-boundary plane. So, for this material, minimum-angle axis–angle pairs were compared with Σ values up to 19, for c/a values between 1.581 and 1.620. In Figs 4a and b all the axis–angle pairs are plotted for type I contrast and type II contrast, respectively, while in Fig. 4c the CSL

orientations from Table I are plotted. It can be seen that the CSLs occupy well-defined positions in the standard triangle, but that there are none that correspond to the axis–angle pairs associated with type I or II contrast. It is thus apparent that there is no systematic correlation between the type of contrast observed and the type of the grain boundary according to the CSL criteria.

Fig. 5 is a histogram of the angles between the nearest ⟨10.0⟩-type close-packed directions in the two adjacent grains. It would appear that there is a somewhat sharper distribution in the case of type I contrast (Fig. 5a) than type II (Fig. 5b), with a preponderance of angles just below 30°.

TABLE I Σ values for hexagonal crystals with values of c/a close to that of zinc oxide, for which $c/a = 1.602$

Σ	Axis	Angle (deg)	c/a
7	[0 0 1]	21.79	All
13	[0 0 1]	27.8	All
19	[0 0 1]	13.17	All
7	[2 1 0]	64.62	1.581
11	[2 1 0]	35.1	1.581
11	[1 0 0]	84.78	1.581
13	[1 0 0]	57.42	1.581
13	[2 1 0]	76.66	1.581
17	[1 0 0]	40.12	1.581
17	[5 1 0]	79.84	1.581
19	[5 0 1]	65.1	1.581
19	[2 1 0]	86.98	1.581
13	[1 0 0]	85.59	1.604
17	[1 0 0]	49.68	1.604
18	[2 1 0]	63.61	1.612
9	[1 0 0]	56.25	1.62
13	[2 1 0]	85.59	1.62
15	[1 0 0]	29.93	1.62
15	[1 0 0]	86.18	1.62
17	[2 1 0]	49.68	1.62

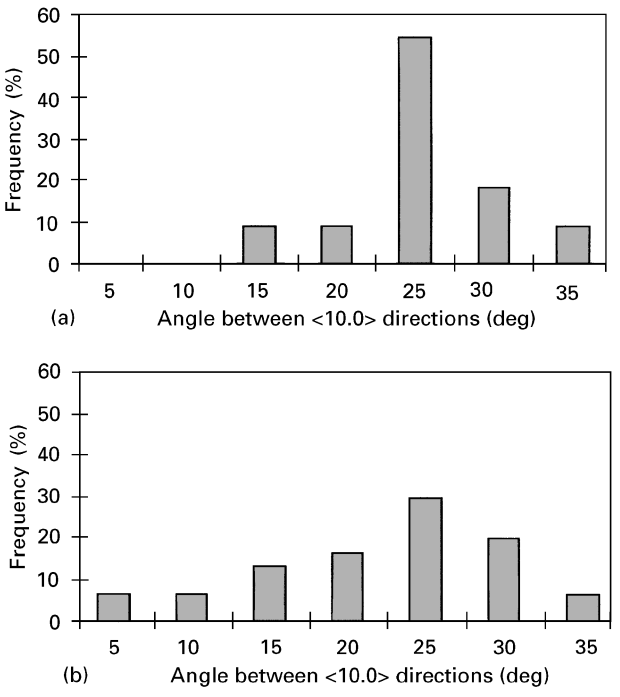

Figure 5 Frequency of angles between the close-packed ⟨10.0⟩ directions of grain boundaries of (a) type I and (b) type II.

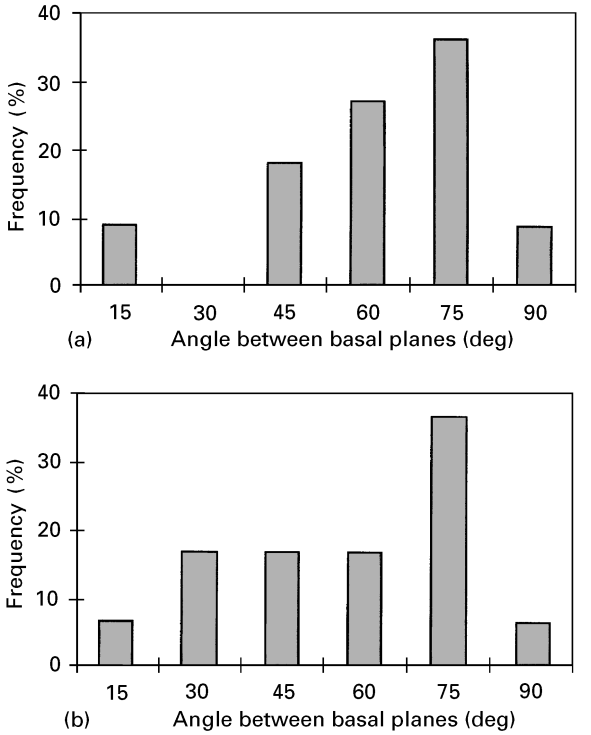

Figure 6 The angle between the basal planes for grain boundaries showing (a) type I contrast and (b) type II contrast.

Fig. 6 shows the angle between the {00.1} (basal) planes of the two grains of type I and type II grain boundaries. Both show a broad distribution of different angles, although it is interesting to note a peak at small angles for the type I boundaries.

We see that these distributions are not random, and in particular there are differences between the distributions for type I and type II boundaries. However, there is no correlation with CSL misorientations; so, although there is some preference for certain crystallography, the relationship is not controlled by CSLs. It thus seems likely that other crystallographic effects are involved, perhaps involving the grain boundary plane. Work is currently in progress to assess this.

5. Conclusions

The correlation of grain-boundary misorientation and the type of CM contrast observed at grain boundaries in additive-free zinc oxide has been studied. The different contrast types were not explained by CSL theory and, in fact, few grain boundaries corresponded to low-multiplicity grain boundaries. Other crystallographic measures such as the basal plane mismatch, and the angle between the closest close-packing directions indicate that there is some degree of crystallographic control of grain-boundary electrical properties in zinc oxide. More detailed analysis will require the full determination of the grain-boundary plane.

References

1. T. K. GUPTA, *J. Amer. Ceram. Soc.* **73** (1990) 1817.
2. J. D. RUSSELL, D. C. HALLS and C. LEACH, *J. Mater. Sci. Lett.* **14** (1995) 676.
3. *Idem.*, *Acta Mater.* **44** (1996) 2431.
4. M. H. BERGER and J. Y. LAVAL, *J. Phys., Paris, Colloque C*, (1990) C1-99.
5. X. J. WU, V. SZKIELKO and P. HAASEN, *J. Phys. Paris, Colloque C*, (1982) C1-135.
6. A. BARY, B. MERCEY, G. POULLAIN, J. L. CHERMANT and G. NOUET, *Rev. Phys. Appl.* **22** (1987) 597.
7. G. POULLAIN, B. MERCEY and G. NOUET, *J. Appl. Phys.* **61** (1987) 1547.
8. D. J. DINGLEY, L. BAKER and L. HUNNINGS, "Electron microscopy and analysis 1981", Institute of Physics Conference Series, Vol. 61 (Institute of Physics, Bristol, 1982) p. 541.
9. B. RAZA and D. B. HOLT, Institute of Physics Conference Series, Vol. 146 (Institute of Physics, Bristol, 1995) p. 107.
10. D. H. WARRINGTON, *J. Phys., Paris, Colloque C4, Suppl.* 10, **36** (1975) C4-87.
11. D. G. BRANDON, *Acta Metall.* **14** (1966) 1479.
12. R. BONNET, E. COUSINO and D. H. WARRINGTON, *Acta Crystallogr. A* **37** (1981) 184.
13. H. GRIMMER, *Acta Crystallogr. A* **45** (1989) 320.

Received 23 July 1996
and accepted 20 January 1997